Assessing Alkyl-, Silyl-, and Halo-Substituent Effects on the Electron Affinities of Silyl Radicals

Joseph D. Larkin,[†] Charles W. Bock,[‡] and Henry F. Schaefer III*,[†]

Center for Computational Chemistry, University of Georgia, Athens, Georgia 30602, and School of Science and Health, Department of Chemistry, Philadelphia University, Philadelphia, Pennsylvania 19144

Received: May 10, 2005; In Final Form: August 5, 2005

Neutral anion energy differences for a large class of α-substituted silyl radicals have been computed to determine the effect of alkyl, silyl, and halo substituents on their electron affinities. In particular, we report theoretical predictions of the adiabatic electron affinities (AEAs), vertical electron affinities (VEAs), and vertical detachment energies (VDEs) for a series of methyl-, silyl-, and halo-substituted silyl radical compounds. This work utilizes the carefully calibrated DZP++ basis set (Chatgilialoglu, C. *Chem. Rev.* **2002**, *102*, 231), in conjunction with the pure BLYP and OLYP functionals, as well as with the hybrid B3LYP, BHLYP, PBE1PBE, MPW1K, and O3LYP functionals. Bromine has the largest effect in stabilizing the anions, and the BLYP/DZP++ AEA for $SiBr_3$ is 3.29 eV. The other predicted electron affinities are for SiH_3 (1.37 eV), SiH_2CH_3 (1.09 eV), SiH_2F (1.54 eV), SiH_2Cl (1.94 eV), SiH_2Br (2.05 eV), $SiH_2(SiH_3)$ (1.77 eV), $SiH(CH_3)_2$ (0.92 eV), $SiHF_2$ (1.86 eV), $SiHCl_2$ (2.53 eV), $SiHBr_2$ (2.67 eV), $Si(CH_3)_3$ (0.86 eV), SiF_3 (2.66 eV), $SiCl_3$ (3.21 eV), $Si(SiH_3)_3$ (2.25 eV), and SiFClBr (3.13 eV). For the five silyl radicals where experimental data are available, the BLYP functional gives the most accurate determination of AEAs; the average absolute error is 0.04_1 eV, whereas the corresponding errors for the O3LYP, MPW1K, PBE1PBE, B3LYP, OLYP, and BHLYP functionals are 0.05_8, 0.06_0, 0.06_3, 0.08_5, 0.11_5, and 0.15_3 eV, respectively.

I. Introduction

Recently, high concentrations of very reactive silyl radicals have been observed in silane plasmas, clearly demonstrating their importance in chemical vapor deposition(CVD) processes.[1] Indeed, SiH_3 radicals are the dominant reactive species in the production of a variety of high-temperature structural materials, including ceramics.[2] Silyl radicals also play a central role in the free-radical hydrosilation of poly(phenylsilane); this process has applications in the fields of photoconducting materials, microlithography, and nonlinear optics.[3] Although little is currently known about how to employ silyl radicals effectively in organic synthesis, the boom in carbon-based radical-driven synthetic reactions, in conjunction with the ability of silyl radicals to form stereoselective bonds, may provide the driving force needed to popularize these radicals soon.[4] Silyl radical anions (these are closed-shell systems) are typically employed to generate silicon−carbon bonds,[5,6] and they act as nucleophiles, analogous to their carbon counterparts. Applications involving these anions include the preparation of acylsilanes in sugar chemistry (via copper catalysis reactions with acyl halides[4]) and the production of bioactive compounds that are synthetically equivalent to amino aldehydes.[7]

Computations have already successfully characterized a large set of atomic and molecular electron affinities,[8] substituent effects on methyl radicals,[9] and substituent effects on silyl- and carbanion stability.[5] In this research, we assess the extent to which silyl and halogen substituents impact the structures, energetics, and electron affinities of silyl radicals. In our continuing efforts[8] to calibrate DFT functionals for the accurate determination of electron affinities, we have also included here computations with the more recently developed OLYP, O3LYP, PBE1PBE, and MPW1K functionals in those cases where experimental data is available. In addition, we discuss the inverse relationship between electronegativities and electron affinities of silyl radicals and compare to earlier analogous work on methyl radicals[9] and silylenes.[10]

II. Theoretical Methods

Equilibrium geometries and vibrational frequency analyses for all the radicals and anions in this study were predicted using generalized gradient approximation (GGA) exchange correlation density functionals, as well as two HF/DFT hybrid functionals. The three "standard" functionals are designated BLYP, B3LYP, and BHLYP, respectively, representing the pure DFT exchange functional (B),[11] a three-parameter HF/DFT hybrid exchange functional (B3),[12] and a modified half-and-half HF/DFT hybrid method (BH),[13] all coupled with the dynamical correlation functional of Lee, Yang, and Parr (LYP).[14] In addition, for the five species of silyl radicals where reliable experimental electron affinities are available, we employed the pure OLYP and hybrid O3LYP functionals. These functionals incorporate the novel OPTX local exchange functional of Handy, Cohen, and coworkers[15,16] the hybrid PBE1PBE[17,18] functional, which utilizes the one-parameter GGA PBE[19] functional and the MPW1K functional. The latter is constructed from a modified version of the Perdew−Wang gradient-corrected exchange functional (MPW)[20] and has been parametrized specifically for kinetics.[21] All DFT computations were carried out using the GAUSSIAN 94,[22] 98,[23] and 03[24] suite of programs.

Double-ζ quality basis sets with polarization and diffuse functions (DZP++) were used throughout for geometry optimizations and vibrational frequency analyses. The DZP++ basis sets were constructed from the Huzinaga−Dunning−Hay[25−27] sets of contracted Gaussian functions. A set of p-type polarization functions for each hydrogen atom was added, and one set

* Author to whom correspondence should be addressed.
[†] University of Georgia.
[‡] Philadelphia University.

10.1021/jp052439p CCC: $30.25
Published on Web 10/19/2005

of five d-type polarization functions was included on each heavy atom. Basis functions for bromine were obtained from the standard Ahlrichs' double-ζ spd set[28] with one set of more extended d-like polarization functions [α_d (Br) = 0.389]. These basis sets were further augmented with diffuse functions; each atom received one additional s-type and one additional set of p-type functions. The diffuse orbital exponents were determined in an even-tempered sense according to the prescription set forth by Lee and Schaefer:[29]

$$\alpha_{\text{diffuse}} = \frac{1}{2}\left(\frac{\alpha_1}{\alpha_2} + \frac{\alpha_2}{\alpha_3}\right)\alpha_1$$

where α_1, α_2, and α_3 are the three smallest Gaussian orbital exponents of the s- or p-type primitive functions for a given atom ($\alpha_1 < \alpha_2 < \alpha_3$). The added diffuse functions have orbital exponents $\alpha_s(H) = 0.04415$, $\alpha_s(C) = 0.04302$, $\alpha_p(C) = 0.03629$, $\alpha_s(Si) = 0.02729$, $\alpha_p(Si) = 0.025$, $\alpha_s(F) = 0.1049$, $\alpha_p(F) = 0.0826$, $\alpha_s(Cl) = 0.05048$, $\alpha_p(Cl) = 0.05087$, $\alpha_s(Br) = 0.0469096$, and $\alpha_p(Br) = 0.0465342$. The final contraction schemes were as follows: H(5s1p/3s1p), C(10s6p1d/5s3p1d), Si(13s9p1d/7s5p1d), F(10s6p1d/5s3p1d), Cl(13s9p1d/7s5p1d), and Br(15s12p6d/9s7p3d). To benchmark the DFT methods employed in this study, more rigorous CCSD(T)[30,31] computations were carried out on SiH_3 with the five silicon core orbitals frozen and no restriction on excitation into the virtual space. These SiH_3 CCSD(T) computations were carried out in conjunction with the Dunning−Woon aug-cc-pVQZ[32,33] basis set. For SiH_2F, with the aug-cc-pCVTZ[34] basis set, we correlated all electrons and placed no restriction on the virtual orbitals. All CCSD(T) computations were performed using the ACESII[35] suite of programs.

The three types of neutral anion energy differences reported in this article were evaluated as differences of total energies: the adiabatic electron affinity

$$\text{AEA} = E(\text{optimized neutral}) - E(\text{optimized anion})$$

the vertical electron affinity

$$\text{VEA} = E(\text{optimized neutral}) - E(\text{anion at optimized neutral geometry})$$

and the vertical detachment energy of the anion

$$\text{VDE} = E(\text{neutral at optimized anion geometry}) - E(\text{optimized anion})$$

III. Results and Discussion

Selected equilibrium geometries are presented in Figures 1−3, with the remainder shown in the Supporting Information. The ground electronic states of all the neutral silyl radicals in this work are doublets, whereas the corresponding anions are closed-shell singlets. The computed values of the AEA, VEA, and VDE were corrected for the zero-point vibrational energy and are listed in Tables 1−3 respectively; experimental values of the AEA, where available, are given in Table 1.

III.A. SiH_3 and SiH_3^-. Equilibrium geometries for the $^2A_1$ ground state of SiH_3 and the corresponding $^1A_1$ ground state of SiH_3^- are shown in Figure 1; for SiH_3, the spin densities clearly indicate that its unshared electron is located primarily on the Si atom. All the functionals employed in this study overshoot both the Si−H bond distance and the H−Si−H bond angle of SiH_3 compared to the proposed experimental values,[36] 1.46 ± 0.01 Å and 110 ± 2°. A similar tendency was reported by Pak et al.[37] in a prior investigation of unsubstituted silicon hydrides. It should be noted, however, that these DFT results are in good agreement with our high-level CCSD(T)/aug-cc-pVQZ results, where the computed Si−H bond length, 1.481 Å, and H−Si−H bond angle, 111.3°, are also greater than the analogous

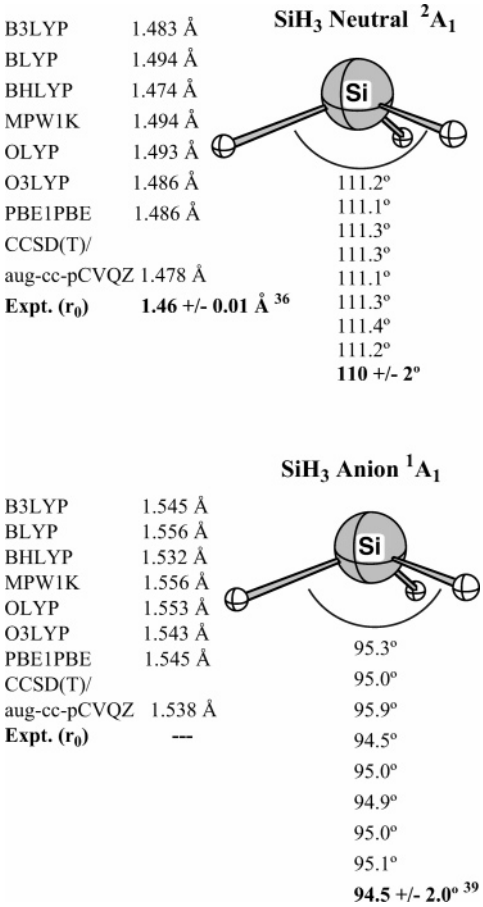

Figure 1. Equilibrium geometries for the $^2A_1$ state of the radical SiH_3 and the $^1A_1$ state of the SiH_3^- anion.

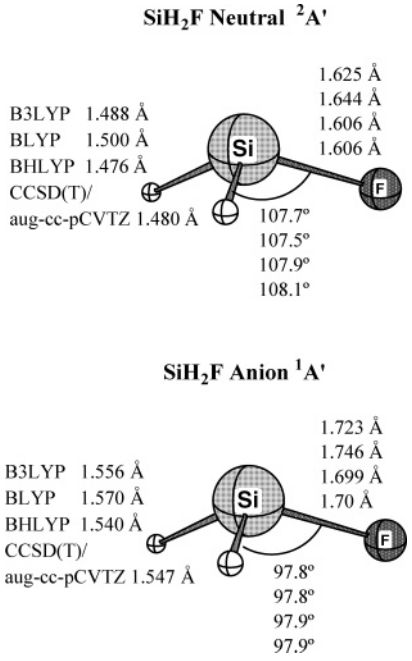

Figure 2. Equilibrium geometries for the $^2A'$ state of the radical SiH_2F and the $^1A'$ state of the SiH_2F^- anion.

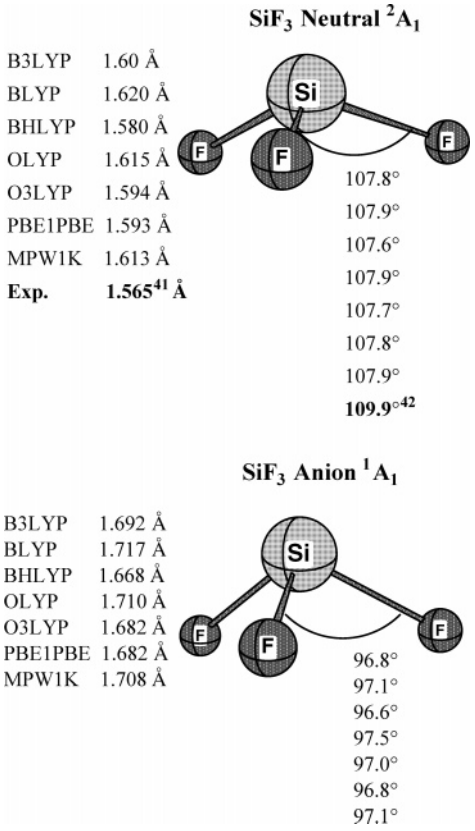

Figure 3. Equilibrium geometries for the $^2A_1$ state of the SiF_3 radical and the $^1A_1$ state of the SiF_3^- anion.

experimental values. Of the functionals employed in this study, BHLYP predicts the shortest Si−H distance for SiH_3, 1.474 Å, although it is still 0.006 Å longer than the experimental r_o value. The newer OLYP, O3LYP, PBE1PBE, and MPW1K functionals all give geometrical parameters for SiH_3 that are similar to those from the conventional BLYP, B3LYP, and BHLYP functionals (see Figure 1).

There are considerable changes in both the experimental and computed structures of SiH_3 upon the addition of an electron. In particular, the H−Si−H bond angle decreases sharply from its nearly tetrahedral value of ∼111° in SiH_3 to a more steeply pyramidal value of ∼95° for SiH_3^-, see Figure 1. This decrease is primarily a result of doubly occupying a nonbonding orbital that has substantial s-character;[38] indeed, NBO analysis suggests that this lone-pair Kohn−Sham orbital has ∼50% s-character. Our optimizations also predict that the additional electron in SiH_3^- results in an increase in the length of the Si−H bonds by ∼0.06 Å. This increase helps alleviate the effects of hydrogen repulsion that would otherwise increase as the H−Si−H angle decreases.

The adiabatic electron affinities computed for SiH_3 in this study differ by as much as 0.23 eV, see Table 1; the MPW1K (1.44 eV), B3LYP (1.45 eV), and BLYP (1.37 eV) functionals provide the best agreement with the experimental value, 1.406 ± 0.014 eV, as determined by photoelectron spectroscopy.[39] It should be noted that our more rigorous CCSD(T)/aug-cc-pVQZ computations predict the AEA value to be 1.38 eV.

III.B. SiH_2CH_3, SiH_2SiH_3, SiH_2F, SiH_2Cl, SiH_2Br, and Their Anions. We first consider the monosubstituted silyl radicals SiH_2CH_3, SiH_2F, SiH_2Cl, SiH_2Br, SiH_2SiH_3, and their associated anions. Structures from our DFT optimizations of SiH_2F are shown in Figure 2, while those of the other monosubstituted species are given in the Supporting Information. Unfortunately, there are no experimental structural data available for any of these monosubstituted species. Our computations predict that replacement of one of the hydrogen atoms with a fluorine atom results in only an ∼0.01 Å elongation of the two remaining Si−H distances, while the H−Si−H angle increases by ∼3.5°, see Figure 2. The predicted Si−H and Si−X (X = F, Cl, Br) distances using the BHLYP functional are consistently shorter than the corresponding distances using either the BLYP or the B3LYP functionals; see the Supporting Information.

Examination of Table 1 for these monosubstituted silyl radicals shows distinct trends in the computed values of the AEA compared to that of SiH_3. For example, for the BLYP functional, $-CH_3$ substitution decreases the AEA by 0.28 eV, whereas $-SiH_3$, −F, −Cl, and −Br substitution increase it by 0.40, 0.17, 0.57, and 0.68 eV, respectively. For the anions in this group of compounds photodetachment data[38] is available only for $SiH_2CH_3^-$, and the resulting experimental value of the AEA, 1.01 ± 0.03 eV, is nearly 0.40 ± 0.04 eV (28 ± 3%) lower than the corresponding experimental value for SiH_3. For comparison, we note that the computed values of AEA for SiH_2CH_3 are roughly 0.3 eV (∼22%) less than the corresponding theoretical values for SiH_3.[39] Although the average difference between the magnitude of the experimental and computed values of SiH_2CH_3 is relatively large, 0.08 ± 0.05 eV, the O3LYP and PBE1PBE functionals perform very well, with predicted values of 1.02 and 1.04 eV, respectively. It should be noted that the BHLYP functional consistently predicts the lowest value of AEA for all the monosubstituted silyl radicals in this study; this is also the case for multiple substitutions, see Table 1. Our experience with this functional on a large set of compounds[8] suggests that it typically provides lower bounds to experimental AEA results.

Although no experimental electron affinity data is available for SiH_2F or SiH_2Cl, our theoretical AEA values obtained from various DFT methods are in reasonable accord with those computed for these compounds by Rodriquez and Hopkinson[40] using isogyric reactions at the MP4/6-311++G(d,p)//HF/6-311++G(d,p) and MP4/6-311++G(2df,p)//HF/6-311++G(d,p) computational levels. Our BHLYP value of 1.40 eV for SiH_2F and our BLYP value of 1.94 eV for SiH_2Cl are in particularly good agreement with their results. We also carried out computations of the AEA for SiH_2F at the CCSD(T)/aug-cc-pCVTZ level, and the predicted value of 1.46 eV is also in good agreement with the predicted value of Rodriquez and Hopkinson.[40] Our BHLYP computed Si−H bond length, 1.476 Å, and bond angle, 107.9°, are in excellent agreement with the corresponding CCSD(T) values of 1.480 Å and 108.1°, respectively.

III.C. $SiH(CH_3)_2$, $SiH(SiH_3)_2$, $SiHF_2$, $SiHCl_2$, $SiHBr_2$, and Their Anions. Optimized structures of all the disubstituted radicals and their anions may be found in the Supporting Information. In accord with our observations from the previous section, the trend in electron affinities for these radicals follows a similar pattern. For example, for the BLYP functional, substitution with a second $-CH_3$ group lowers the predicted values of the AEA compared to that of $SiH_2(CH_3)$ by 0.17 eV. Substitution with a second $-SiH_3$, −F, −Cl, or −Br group increase the AEA values by 0.28, 0.32, 0.59, or 0.62 eV, respectively, when compared to that of the corresponding monosubstituted radical. For the disubstituted silyl radicals, the only experimental electron affinity from the literature is for $SiH(CH_3)_2$; interestingly, the value of AEA, 0.91 ± 0.02[5] eV, is only 0.1 eV (∼9.9%) smaller than the experimental value for $SiH_2(CH_3)$. Thus, the observed decrease in the AEA value in

TABLE 1: DFT/DZP++ and Experimental Adiabatic Electron Affinities (AEA) in eV

	B3LYP	BLYP	BHLYP	OLYP	O3LYP	PBE1PBE	MP1WK	exptl
SiH_3[a]	1.45	1.37	1.22	1.24	1.33	1.34	1.44	1.406 ± 0.014[b]
SiH_2CH_3	1.16	1.09	0.93	0.95	1.02	1.04	1.14	1.01 ± 0.03[c]
SiH_2F[d,e]	1.63	1.54	1.40					
SiH_2Cl[f]	2.04	1.94	1.85					
SiH_2Br	2.16	2.05	1.97					
$SiH_2(SiH_3)$	1.85	1.77	1.61					
$SiH(CH_3)_2$	0.98	0.92	0.74	0.78	0.83	0.84	0.95	0.91 ± 0.02[g]
$SiHF_2$[h]	1.95	1.86	1.73					
$SiHCl_2$	2.64	2.53	2.43					
$SiHBr_2$	2.80	2.67	2.63					
$SiH(SiH_3)_2$	2.13	2.05	1.89					
$Si(CH_3)_3$	0.90	0.86	0.65	0.72	0.76	0.74	0.86	0.824 ± 0.02[e]
SiF_3	2.73	2.66	2.50	2.43	2.51	2.52	2.63	2.41 ± 0.22[i]
$SiCl_3$	3.31	3.21	3.10					
$SiBr_3$	3.41	3.29	3.24					
$Si(SiH_3)_3$	2.34	2.25	2.10					
SiFClBr	3.24	3.13	3.03					

[a] CCSD(T)/aug-cc-pVQZ 1.38 eV. [b] Ref 39. [c] Ref 38. [d] CCSD(T)/aug-cc-pCVTZ 1.46 eV. [e] MP4/6-311++G(d,p)//HF/6-311G(d,p) 1.39 eV (ref 40). [f] MP4/6-311++G(d,p)//HF/6-311G(d,p) 1.94 eV (ref 40). [g] Ref 5. [h] MP4/6-311++G(d,p)//HF/6-311G(d,p) 1.82 eV (ref 40). [i] Ref 45.

TABLE 2: DFT/DZP++ Vertical Electron Affinities (VEA) in eV

	B3LYP	BLYP	BHLYP	OLYP	O3LYP	PBE1PBE	MPW1K
SiH_3	0.96	0.88	0.72	0.76	0.85	0.84	0.94
SiH_2CH_3	0.61	0.55	0.37	0.42	0.49	0.48	0.58
SiH_2F	1.02	0.96	0.77				
SiH_2Cl	1.29	1.21	1.06				
SiH_2Br	1.39	1.31	1.17				
$SiH_2(SiH_3)$	1.20	1.11	0.96				
$SiH(CH_3)_2$	0.37	0.34	0.11	0.22	0.25	0.22	0.35
$SiHF_2$	1.27	1.23	1.01				
$SiHCl_2$	1.71	1.65	1.47				
$SiHBr_2$	1.90	1.84	1.67				
$SiH(SiH_3)_2$	1.40	1.31	1.17				
$Si(CH_3)_3$	0.31	0.32	0.01	0.21	0.22	0.13	0.29
SiF_3	2.69	1.90	1.63	1.70	1.75	1.69	1.86
$SiCl_3$	2.26	2.24	1.98				
$SiBr_3$	2.49	2.46	2.22				
$Si(SiH_3)_3$	1.58	1.49	1.35				
SiFClBr	2.24	2.22	1.95				

TABLE 3: DFT/DZP++ Vertical Detachment Energies (VDE) in eV

	B3LYP	BLYP	BHLYP	OLYP	O3LYP	PBE1PBE	MPW1K
SiH_3	1.91	1.81	1.68	1.68	1.79	1.83	1.91
SiH_2CH_3	1.65	1.56	1.43	1.42	1.51	1.54	1.63
SiH_2F	2.13	2.02	1.93				
SiH_2Cl	2.73	2.58	2.57				
SiH_2Br	2.84	2.67	2.71				
$SiH_2(SiH_3)$	2.46	2.37	2.23				
$SiH(CH_3)_2$	1.48	1.39	1.26	1.24	1.32	1.35	1.44
$SiHF_2$	2.47	2.33	2.29				
$SiHCl_2$	3.40	3.21	3.29				
$SiHBr_2$	3.52	3.29	3.45				
$SiH(SiH_3)_2$	2.82	2.71	2.57				
SiF_3	3.45	3.32	3.27	3.09	3.20	3.26	3.31
$SiCl_3$	4.15	3.96	4.03				
$SiBr_3$	4.13	3.91	4.19				
$Si(SiH_3)_3$	3.05	2.92	2.81				
$Si(CH_3)_3$	1.37	1.29	1.16	1.13	1.20	1.24	1.32
SiFClBr	4.04	3.85	3.94				

going from $SiH_2(CH_3)$ to $SiH(CH_3)_2$ is nearly a factor of 2 smaller than that predicted from our DFT results. The magnitude of the computed values for $SiH(CH_3)_2$ differ from experiment by 0.08 ± 0.05 eV on average, which is similar to what we found for $SiH_2(CH_3)$. The BLYP functional gives an AEA value of 0.92 eV for $SiH(CH_3)_2$, which is indistinguishable from the experimental result (see Table 1). For $SiHF_2$, the computed value of the AEA at the BLYP, 1.86 eV, is very close to the MP4/6-311++G(d,p)//HF/6-311++G(d,p) result of Rodiquez and Hopkinson,[40] 1.82 eV.

III.D. $Si(CH_3)_3$, $Si(SiH_3)_3$, SiF_3, $SiCl_3$, $SiBr_3$, and Their Anions. Equilibrium geometries for the $^2A_1$ ground electronic state of the SiF_3 neutral radical and the corresponding $^1A_1$ closed-shell anion are presented in Figure 3; geometries of the other trisubstituted species are given in the Supporting Information. Tanimoto and Saito[41] have reported a microwave structure

TABLE 4: Changes in the BLYP/DZP++ AEAs, Using SiH_3 as a Point of Reference

Effect on the AEA of SiH_3 from Each Substituent	
SiH_3	0.00[a]
SiH_2CH_3	−0.28
$SiH(CH_3)_2$	−0.4
$Si(CH_3)_3$	−0.51
SiH_2SiH_3	0.40
$SiH(SiH_3)_2$	0.68
$Si(SiH_3)_3$	0.88
SiH_2F	0.17
$SiHF_2$	0.49
SiF_3	1.29
SiH_2Cl	0.57
$SiHCl_2$	1.16
$SiCl_3$	1.84
SiH_2Br	0.68
$SiHBr_2$	1.30
$SiBr_3$	1.92

[a] The actual predicted AEA of SiH_3 is 1.37 eV.

for SiF_3; the Si−F bond length is deduced to be 1.565 Å, when the F−Si−F bond angles are assumed to be 109.9°, from the IR matrix isolation study of Milligan et al.[42] As noted previously, the functionals in this study typically overshoot the Si−X (X = H, F) bond lengths when compared to experiment, and for SiF_3 the predicted Si−F distances are from 0.015 to 0.055 Å longer than the infrared/microwave result. On the other hand, the F−Si−F bond angle, in contrast to the H−Si−H angle in SiH_3, is less than the experiment by 2.0−2.3°. Again, the BHLYP functional predicts a structure that is closest in agreement to experiment, see Figure 3. Our DFT optimizations predict a significant change in the structure of the neutral SiF_3 radical upon the addition of an electron. The F−Si−F angle decreases dramatically, on average by 10.8°, and this is accompanied by an increase in the Si−F bond length of ∼0.09 Å; this increase in bond length reduces the effects of fluorine substitution in this compound.

In accord with an observation made by Wetzel et al.,[38] we note that methyl substitution is not additive in the sense that, the large decrease, 0.4 eV (experimental), 0.3 eV (theoretical), in the AEA in going from SiH_3 to $SiH_2(CH_3)$ is followed by a much smaller reduction, 0.2 eV (experimental), 0.1 eV (theoretical), in going from $SiH_2(CH_3)$ to $SiH(CH_3)_2$. Replacing the final H atom with a methyl group results in an even smaller reduction in the AEA, see Table 4. This trend was also noted by Frenking et al. for AX_3^+ and AH_2X^+ systems (A = C, Si, Ge, Sn, Pb; X = F, Cl, Br, I).[43]

It is evident from Tables 1−3 that for mono-, di-, and trisubstituted silyl radicals the electron affinity consistently depends on the substituents in the order CH_3 < H < F < SiH_3 < Cl < Br. The rate of increase in electron affinity for the halo and silyl substituents is also shown in Table 4. These results are consistent with those found for the electron affinities of methyl radicals and silylenes,[9,10] where a similar inverse relationship between the electronegativity of a substituent and its corresponding electron affinity was observed.

An explanation of this trend for the halogenated silyl radicals relies on the fact that flourine is a weaker π-donor than the other halogens. Frenking and co-workers[43] showed that for halogens, the π-donor ability increases with F < Cl < Br < I for both cations and neutral molecules, and this increase in electron density causes silicon to become a much stronger electron attractor. Interestingly enough, the same effect can be seen among the relationship between methyl and silyl substituents due in part to the electropositive nature of silicon[38,44] as well as the π-back-donation described by Frenking et al.[43] This rationalization can also be extended to the inverse relationship of electron affinities and electronegativities observed previously[9,10] for the divalent CX_2 and SiX_2 molecules (X = CH_3, SiH_3, F, Cl, and Br).

III.E. Performance of Newer Functionals. Considering the wealth of new functionals[15−19] being reported in the literature and in view of our ongoing research effort to find efficient, accurate methods to predict electron affinities, we have considered four of the more recently developed functionals to assess their ability to predict EAs. Unfortunately, only limited experimental data is available to compare with for the silyl radicals discussed in this work.

For the parent SiH_3 radical, the MPW1K functional performs better than the other newer OLYP, O3LYP, and PBE1PBE functionals, as well as the exhaustively tested BLYP, B3LYP, and BHLYP functionals, providing the closet agreement to the experimental value.[39] The MPW1K functional has an interesting property: for the five silyl radicals where experimental data is available, the predicted AEAs from this functional are all greater than the observed values. If this property persists on a more comprehensive database, the MPW1K functional may prove useful in generating upper bounds on AEA values. The B3LYP functional also appears to have the same general property.[8]

Although the O3LYP functional performs better than all the other functionals in predicting the AEA of SiH_2CH_3 (see Table 1), its performance is erratic in that in some cases it gives AEA values greater than experiment, while in other cases it gives values less than experiment. Interestingly, AEA values obtained from O3LYP are consistently lower than those from B3LYP; similarly AEA(OLYP) < AEA(BLYP).

For both $SiH(CH_3)_2$ and $Si(CH_3)_3$ the best agreement with experiment is obtained using the well-tested BLYP functional. However, the predicted AEA values from the OLYP, O3LYP, and PBE1PBE functionals are only ∼0.10 to 0.15 eV too low. Furthermore, for all four of the newer functionals AEA($Si(CH_3)_3$) < AEA($SiH(CH_3)_2$), which is consistent with experiment.[38]

In the case of SiF_3, the OLYP functional gives an AEA value that is closest to experiment. However, the uncertainty associated with the experimental electron affinity of SiF_3, ±0.22[45] eV, is quite large, making it difficult to determine which functional gives results closest to experiment. Indeed, only two of our computed AEA values actually fall outside the reported error. It should also be noted that the BHLYP and OLYP functionals give values of AEA that are below the experimental values for SiH_3, $SiH_2(CH_3)$, $SiH(CH_3)_2$, and $Si(CH_3)_3$ but above that for SiF_3. This could indicate that the experimental value of 2.41 eV for SiF_3 may be somewhat low. In view of these limitations in the experimental result for SiF_3, particularly the large error bars (which are nearly an order of magnitude greater than that associated with the other experimental EAs), we have excluded the AEA of SiF_3 in our assessment of average absolute errors. For the ensemble of silyl radicals studied in this work, DZP++ BLYP provides the most accurate computations of electron affinities—the average absolute error is only about four-hundredths of an eV. BLYP has been shown previously to provide excellent results for a large set of compounds.[8] The average errors in increasing order are as follows: BLYP (0.04_1) < O3LYP (0.05_8) < MPW1K (0.06_0) < PBE1PBE (0.06_3) < B3LYP (0.08_5) < OLYP (0.11_5) < BHLYP (0.15_3). Although the results presented in this article are less than exhaustive, the performance of the O3LYP, MPW1K, and PBE1PBE function-

als in computing AEAs is encouraging. Further testing on a more diverse collection of compounds is clearly required to assess the performance these functionals in computing EAs.

IV. Conclusions

Substituted silyl radicals were examined in this research to characterize the effect that alkyl and halo substituents have on the magnitude of electron affinities, as well as to provide an ensemble of molecules to gauge the accuracy of several newer pure (OLYP) and hybrid (O3LYP, MPW1K, PBE1PBE) density functionals for future electron affinity studies. An inverse relationship between electronegativities and electron affinities is found for the silyl radicals in this study, which is consistent with analogous studies of methyl radicals, carbenes, and silylenes.[9,10] This, we assert, is a consequence of back-donation of electron density via π-bonds from the heavier halo substituents. This effect stabilizes the neutral structures and increases their attraction for electrons.[43] Thus, substituents with weak back-donating character, e.g., fluorine, have lower than expected values of the AEA.

Interestingly, the rather old BLYP method[11,14] performed the best of all the functionals in this study in computing AEAs for those silyl radicals where reliable experimental results are available for comparison. However, the more recently developed O3LYP, PBE1PBE, and MPW1K hybrids show promise in this regard, although extensive testing on a more diverse collection of molecules is clearly required. In general, the performance of DFT methods for predicting molecular electron affinities of a variety of structures[9,10] is encouraging, particularly in light of the great difficulty[8] in determining experimental EAs to within ± 0.1 eV.

Acknowledgment. This research was supported by the National Science Foundation, Grant No. CHE-045144.

Supporting Information Available: BLYP and B3LYP structures. This material is available free of charge via the Internet at http://pubs.acs.org.

References and Notes

(1) Chatgilialoglu, C. *Chem. Rev.* **1995**, *95*, 1229.
(2) Tachibana, A.; Yamaguchi, K.; Kawauchi, S.; Kurosaki, Y.; Yamabe, T. *J. Am. Chem. Soc.* **1992**, *114*, 7504.
(3) Hsiao, Y.-L.; Waymouth, R. M. *J. Am. Chem. Soc.* **1994**, *116*, 9779.
(4) Brook, M. A. *Silicon in Organic, Organometallic, and Polymer Chemistry*; John Wiley & Sons: New York, 2000.
(5) Brinkman, E. A.; Berger, S.; Brauman, J. I. *J. Am. Chem. Soc.* **1994**, *116*, 8304.
(6) Colvin, E. W. *Silicon in Organic Synthesis*; Butterworth: London, 1981.
(7) Bonini, B. F.; Comes-Franchini, M.; Fochi, M.; Mazzanti, G.; Ricci, A. *J. Organomet. Chem.* **1998**, *567*, 181.
(8) Rienstra-Kiracofe, J. C.; Tschumper, G. S.; Schaefer, H. F.; Nandi, S.; Ellison, G. B. *Chem. Rev.* **2002**, *102*, 231.
(9) Li, Q.; Zhao, J. F.; Xie, Y.; Schaefer, H. F. *Mol. Phys.* **2002**, *100*, 3615.
(10) Larkin, J. D.; Schaefer, H. F. *J. Chem. Phys.* **2004**, *121*, 9361.
(11) Becke, A. D. *Phys. Rev. A* **1988**, *38*, 3098.
(12) Becke, A. D. *J. Chem. Phys.* **1993**, *98*, 1372.
(13) Becke, A. D. *J. Chem. Phys.* **1993**, *98*, 5648.
(14) Lee, C.; Yang, W.; Parr, R. G. *Phys. Rev. B* **1988**, *37*, 785.
(15) Handy, N. C.; Cohen, A. J. *Mol. Phys.* **2001**, *99*, 403.
(16) Hoe, W.-M.; Cohen, A. J.; Handy, N. C. *Chem. Phys. Lett.* **2001**, *341*, 319.
(17) Ernzerhof, M.; Perdew, J. P.; Burke, K. *Int. J. Quantum Chem.* **1997**, *64*, 285.
(18) Ernzerhof, M.; Scuseria, G. E. *J. Chem. Phys.* **1999**, *110*, 5029.
(19) Perdew, J. P.; Burke, K.; Ernzerhof, M. *Phys. Rev. Lett.* **1996**, *77*, 3865.
(20) Adamo, C.; Barone, V. *J. Chem. Phys.* **1998**, *108*, 664.
(21) Lynch, B. J.; Fast, P. L.; Harris, M.; Truhlar, D. G. *J. Phys. Chem. A* **2000**, *104*, 4811.
(22) Frisch, M. J.; Trucks, G. W.; Schlegel, H. B.; Gill, P. M. W.; Johnson, B. G.; Robb, M. A.; Cheeseman, J. R.; Keith, T.; Petersson, G. A.; Montgomery, J. A.; Raghavachari, K.; Al-Laham, M. A.; Zakrzewski, V. G.; Ortiz, J. V.; Foresman, J. B.; Cioslowski, J.; Stefanov, B. B.; Nanayakkara, A.; Challacombe, M.; Peng, C. Y.; Ayala, P. Y.; Chen, W.; Wong, M. W.; Andres, J. L.; Replogle, E. S.; Gomperts, R.; Martin, R. L.; Fox, D. J.; Binkley, J. S.; Defrees, D. J.; Baker, J.; Stewart, J. P.; Head-Gordon, M.; Gonzalez, C.; Pople, J. A. *GAUSSIAN 94*, revision C.3 ed.; Gaussian, Inc.: Pittsburgh, PA, 1995.
(23) Frisch, M. J.; Trucks, G. W.; Schlegel, H. B.; Scuseria, G. E.; Robb, M. A.; Cheeseman, J. R.; Zakrzewski, V. G.; Montgomery, J. A.; Stratmann, R. E.; Burant, J. C.; Dapprich, S.; Millam, J. M.; Daniels, A. D.; Kudin, K. N.; Strain, M. C.; Farkas, O.; Tomasi, J.; Barone, V.; Cossi, M.; Cammi, R.; Mennucci, B.; Pomelli, C.; Adamo, C.; Clifford, S.; Ochterski, J.; Petersson, G. A.; Ayala, P. Y.; Cui, Q.; Morokuma, K.; Malick, D. K.; Rabuck, A. D.; Raghavachari, K.; Foresman, J. B.; Cioslowski, J.; Ortiz, J. V.; Baboul, A. G.; Stefanov, B. B.; Liu, G.; Liashenko, A.; Piskorz, P.; Komaromi, I.; Gomperts, R.; Martin, R. L.; Fox, D. J.; Keith, T.; Al-Laham, M. A.; Peng, C. Y.; Nanayakkara, A.; Gonzalez, C.; Challacombe, M.; Gill, P. M. W.; Johnson, B. G.; Chen, W.; Wong, M. W.; Andres, J. L.; Head-Gordon, M.; Replogle, E. S.; Pople, J. A. *GAUSSIAN 98*, A.10 ed.; Gaussian, Inc.: Pittsburgh, PA, 1998.
(24) Frisch, M. J.; Trucks, G. W.; Schlegel, H. B.; Scuseria, G. E.; Robb, M. A.; Cheeseman, J. R.; Montgomery, J. A.; Vreven, T.; Kudin, K. N.; Burant, J. C.; Millam, J. M.; Iyengar, S. S.; Tomasi, J.; Barone, V.; Mennucci, B.; Cossi, M.; Scalmani, G.; Rega, N.; Petersson, G. A.; Nakatsuji, H.; Hada, M.; Ehara, M.; Toyota, K.; Fukuda, R.; Hasegawa, J.; Ishida, M.; Nakajima, T.; Honda, Y.; Kitao, O.; Nakai, H.; Klene, M.; Li, X.; Knox, J. E.; Hratchian, H. P.; Cross, J. B.; Adamo, C.; Jaramillo, J.; Gomperts, R.; Stratmann, R. E.; Yazyev, O.; Austin, A. J.; Cammi, R.; Pomelli, C.; Ochterski, J. W.; Ayala, P. Y.; Morokuma, K.; Voth, G. A.; Salvador, P.; Dannenberg, J. J.; Zakrzewski, V. G.; Dapprich, S.; Daniels, A. D.; Strain, M. C.; Farkas, O.; Malick, D. K.; Rabuck, A. D.; Raghavachari, K.; Foresman, J. B.; Ortiz, J. V.; Cui, Q.; Baboul, A. G.; Clifford, S.; Cioslowski, J.; Stefanov, B. B.; Liu, G.; Liashenko, A.; Piskorz, P.; Komaromi, I.; Martin, R. L.; Fox, D. J.; Keith, T.; Al-Laham, M. A.; Peng, C. Y.; Nanayakkara, A.; Challacombe, M.; Gill, P. M. W.; Johnson, B.; Chen, W.; Wong, M. W.; Gonzalez, C.; Pople, J. A. *GAUSSIAN 03*, B.02 ed.; Gaussian, Inc.: Pittsburgh, PA, 2003.
(25) Huzinaga, S. *J. Chem. Phys.* **1965**, *42*, 1293.
(26) Dunning, T. H.; Hay, P. J. *Modern Theoretical Chemistry*; Schaefer, H. F., Ed.; Plenum Press: New York, 1977; Vol. 3, pp 1−27.
(27) Huzinaga, S. *Approximate Atomic Wave functions II*; University of Alberta: Edmonton, Alberta, 1971.
(28) Schafer, A.; Horn, H.; Ahlrichs, R. *J. Chem. Phys.* **1992**, *97*, 2571.
(29) Lee, T. J.; Schaefer, H. F. *J. Chem. Phys.* **1985**, *83*, 1784.
(30) Raghavachari, K.; Trucks, G. W.; Pople, J. A.; Head-Gordon, M. *Chem. Phys. Lett.* **1989**, *157*, 479.
(31) Scuseria, G. E. *Chem. Phys. Lett.* **1991**, *176*, 27.
(32) Dunning, T. H. *J. Chem. Phys.* **1989**, *90*, 1007.
(33) Woon, D. E.; Dunning, T. H. *J. Chem. Phys.* **1993**, *98*, 1358.
(34) Dunning, T. H.; Woon, D. E. *J. Chem. Phys.* **1995**, *103*, 4572.
(35) Stanton, J. F.; Gauss, J.; Watts, J. D.; Lauderdale, W. J.; Bartlett, R. J.; *ACESII*. We thank Professor John Stanton for his help with the ACESII program.
(36) Yamada, C.; Hirota, E. *Phys. Rev. Lett.* **1986**, *56*, 923.
(37) Pak, C.; Rienstra-Kiracofe, J.; Schaefer, H. F. *J. Phys. Chem. A* **2000**, *104*, 11232.
(38) Wetzel, D. M.; Saloman, K. E.; Berger, S.; Brauman, J. I. *J. Am. Chem. Soc.* **1989**, *111*, 3835.
(39) Nimlos, M. R.; Ellison, G. B. *J. Am. Chem. Soc.* **1986**, *108*, 6522.
(40) Rodriquez, C. F.; Hopkinson, A. C. *Can. J. Chem.* **1992**, *70*, 2234.
(41) Tanimoto, M.; Saito, S. *J. Chem. Phys.* **1999**, *111*, 9242.
(42) Milligan, D. E.; Jacox, M. E.; Guillory, W. A. *J. Chem. Phys.* **1968**, *49*, 5330.
(43) Frenking, G.; Fau, S.; Marchaud, C. M.; Grutzmacher, H. *J. Am. Chem. Soc.* **1997**, *119*, 6648.
(44) Weeks, G. H.; Adcock, W.; Klingensmith, K. A.; Waluk, J. W.; West, R.; Vasek, M.; Downing, J.; Michl, J. *Pure Appl. Chem.* **1986**, *58*, 39.
(45) Kawamata, H.; Negishi, Y.; Kishi, R. *J. Chem. Phys.* **1996**, *105*, 5369.